Constitutive relation for the friction between lubricated surfaces

J. M. Carlson and A. A. Batista
Department of Physics, University of California, Santa Barbara, Santa Barbara, California 93106
(Received 25 October 1995)

Motivated by recent experiments and numerical results, we propose a constitutive relation to describe the friction beween two surfaces separated by an atomically thin layer of lubricant molecules. Our phenomenological approach involves the development of a rate and state law to describe the macroscopic frictional properties of the system, in a manner similar to that which has been proposed previously by Ruina [J. Geophys. Res. **88**, 10 359 (1983)] for the solid on solid case. In our case, the state variable is interpreted in terms of the shear melting of the lubricant, and the constitutive relation captures some of the primary experimental differences between the dry and lubricated systems.

PACS number(s): 46.90.+s, 46.30.Pa, 81.40.Pq, 83.20.Bg

I. INTRODUCTION

As mechanical devices become smaller and smaller, an understanding of frictional properties at microscopic scales becomes increasingly important technologically [1]. Of particular interest are the regimes in which the behavior of the small scale system may differ qualitatively from bulk properties [2]. The frictional properties of lubricated interfaces provide an excellent example of such behavior. When two smooth surfaces are separated by a bulk layer of lubricating liquid, e.g., motor oil between the gears of an automobile engine, one typically expects that the lubricant will facilitate the relative motion of the surfaces. That is, first the overall friction will be reduced, and second the surfaces will slide smoothly relative to one another avoiding abrupt and often damaging stick-slip dynamics. In most of these cases, frictional dissipation is well characterized by the bulk viscosity η of the fluid so that the friction force can be written to a good approximation as $F_{\text{bulk}}=\eta V$, where V is the relative velocity of the surfaces. However, the behavior changes substantially when the thickness of the lubricant layer is reduced to atomic dimensions. In this regime, referred to as boundary lubrication, characteristic relaxation times become orders of magnitude greater than those of the bulk [3]. These thin lubricant films can exhibit solidlike properties, including a critical yield stress and a dynamical shear melting transition, which can lead to stick-slip dynamics in certain regimes [4,5].

Recent experiments have made important contributions to our understanding of this phenomenon, both qualitatively and quantitatively. These measurements are made using a surface force apparatus (SFA), the mechanical equivalent of which is illustrated schematically in Fig. 1. The block and the surface on which it slides correspond to two atomically smooth mica surfaces, which are separated by a few molecular layers of lubricant molecules across a contact area roughly 10 μm in diameter. The slider block is attached to one end of a harmonic spring which is pulled at the other end at velocity V. One of the key observations [5] is the existence of a critical pulling velocity V_c which marks the crossover from stick-slip dynamics ($V<V_c$) to continuous sliding at roughly constant velocity ($V>V_c$), an example of which is illustrated in Fig. 2(a).

In this paper we propose a phenomenological constitutive relation which describes the frictional force F_0 on the sliding block as a function of the macroscopic variables which characterize the motion, including position, velocity, and time. In the field of solid mechanics such an approach was introduced by Ruina [6] and has been applied successfully to a wide range of solid on solid systems with roughly micron scale roughness on the surfaces [7,8]. Such equations are referred to as rate and state laws, where the rate variable refers to the sliding velocity, and the state variable is meant to capture all memory dependent effects. In our case, the state variable will represent the degree of melting in the lubricant layer, and the constitutive relation at least qualitatively captures many aspects of the experimental data.

Ultimately the frictional properties of any system are determined by microscopic features such as the contact points between the dry surfaces, or the microscopic forces molecules in a lubricant film exert on the surfaces. The *state* of the system is most directly specified in terms of the microscopic configuration, which in these driven

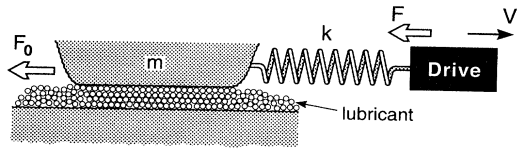

FIG. 1. The mechanical analog of the SFA experimental setup corresponds to a block of mass m connected to an elastic spring of spring constant k which is pulled at one end at velocity V. The block is in contact with a lubricated surface. The surface of the block as well as the sliding surface are composed of atomically smooth mica, and hexadecane is a typical lubricant. The block displacement measured with respect to the stationary lower surface is U, the spring force is $F=-k(U-Vt)$, and the friction force is F_0. The radius of the contact area is of order tens of microns and the thickness of the lubricant is of order 10 Å. Typical drive velocities are in the range 0.001–10 μm/s.

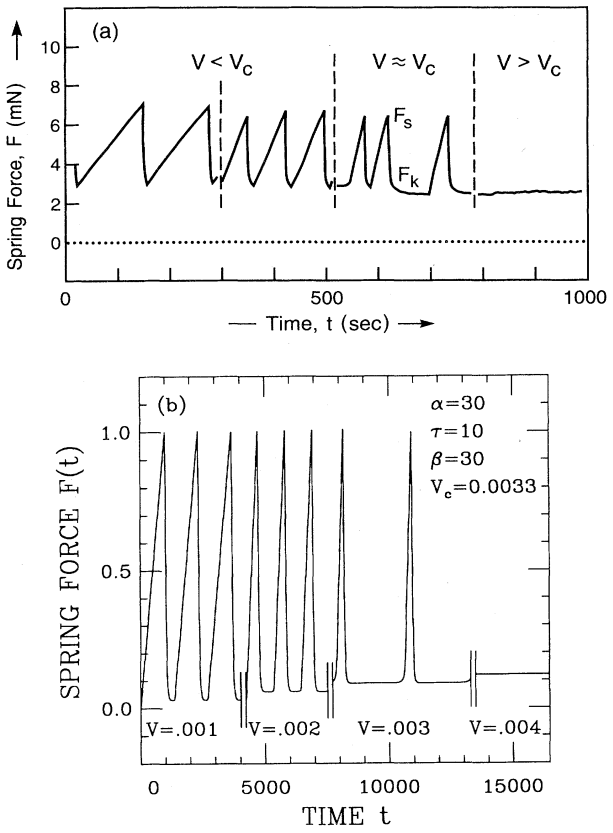

FIG. 2. Traces of the spring force F as a function of time for increasing pulling velocities V. (a) Experimental data from Ref. [5] for a hexadecane film at 17 °C ($T < T_c$) with step increases in velocity V marked by the dotted lines. The critical velocity for this system is $V_c \approx 0.4$ μm/s. (b) Numerical solutions of Eqs. (6)–(8) with the parameter values marked in the figure. In each case there is a discontinuous transition from stick-slip behavior to steady sliding at $V = V_c$, which we take to be the first velocity at which the stick-slip spikes disappear as the velocity is increased in small steps.

systems is a nonequilibrium state. The basic assumption behind the phenomenological rate and state approach is that the microscopic forces are sufficiently self-averaging to produce a macroscopic force law which is deterministic, and depends only on the macroscopic variables which are associated with the motion. In this equation the state variable is associated with a history dependent mean field value, characteristic of some average property of the interface. Ultimately, the goal is to derive the constitutive relation from a microscopic model, and in practice the phenomenological approach is typically the first step towards developing intuition about microscopic models. In fact, some recent progress towards microscopic derivations of rate and state laws has recently been made for the solid on solid case [9].

The remainder of this paper is organized as follows. In Sec. II we provide a summary of relevant experimental and numerical studies of the frictional properties of thin lubricating films. In Sec. III we introduce a rate and state law for boundary lubrication. In Sec. IV we present a series of numerical and analytical solutions of the model in regimes that are designed to mimic experiments. We conclude in Sec. V with a summary of our results and a discussion of some of the important directions for future work.

II. EXPERIMENTS AND NUMERICAL SIMULATIONS

In this section we summarize certain key results from previous experiments by Yoshizawa and Israelachvili [5] along with numerical simulations of Robbins and Thompson [10], and Persson [11] all of which have motivated the constitutive relation that we will introduce in Sec. III.

For systems such as that illustrated in Fig. 1, one of the key experimental observations is a crossover from stick-slip behavior to steady sliding at a critical velocity V_c as illustrated in Fig. 2(a). Yoshizawa and Israelachvili found that the critical velocity can depend on a variety of experimental parameters including the load, the temperature, and the spring constant. Experiments which will determine the dynamical phase diagram for the system are currently in progress [12].

In the stick-slip phase, most of the previous work has focused on systems in which the slip times are much longer than the characteristic period of the mass spring system. Because the slip times are long, these systems are referred to as "overdamped." Such behavior is prevalent for lubricants that consist of complex chain shaped or branched molecules. The alternative "underdamped" behavior, in which slip times are of order $\sqrt{m/k}$, is more common in simpler systems such as the silicone liquid octamethylcyclotetrasiloxane (OMCTS), a spherical molecule. While there are instances in which both underdamped and overdamped responses have been obtained for the same lubricant, such crossovers have not yet been studied systematically.

The generic shape of an overdamped slip pulse is represented in Fig. 2(a). While the block is stuck the spring force rises linearly with time, with a slope given by the product of the spring constant and the pulling speed. When some threshold force is reached, the block abruptly begins to slide, and the spring force relaxes roughly exponentially with time until the block suddenly resticks. Note that an infinitely sharp discontinuity in the slope of the spring force either at the beginning or end of the slip would imply a discontinuity in the velocity of the block. While experimentally the transitions are at least slightly rounded, the clear appearance of sharp changes in Fig. 2 both at the beginning and end of the slip pulse does indicate that the time scales over which the velocity is changing is relatively short. Less obvious in the figure is the fact that the duration of slip appears to increase as the velocity is increased [12]. Intermittent slip pulses have also at times been observed for pulling speeds near V_c. The transition from stick-slip to steady sliding is discontinuous for the overdamped pulses, in some cases with relatively little variation in the amplitude of stick-slip until the transition velocity is reached. In contrast, recent experiments [12] suggest that in the underdamped case the transition is continuous. That is, the stick-slip

amplitude approaches zero continuously as $V \rightarrow V_c$.

The slip pulses that are observed for boundary lubrication are sufficiently different from the generic behavior of dry interfaces [7,13,14] such as those which motivated Ruina's rate and state law, that it is clear that the constitutive laws describing the two classes of systems must be different. Like the overdamped and underdamped pulses described above, for dry interfaces there are also two distinct classes of stick-slip associated with two different time scales [15]. The first consists of inertial pulses, which like the underdamped pulses consist of slips which last a time of order $\sqrt{m/k}$. However, as mentioned above for boundary lubrication the transition in this regime appears to be continuous, while for dry interfaces in this regime the transition is discontinuous [14]. The second case, like the overdamped pulses discussed above, is dominated by a time scale associated with the friction. However, for dry friction the slips start slowly, exhibiting a creeplike behavior until the block is displaced a characteristic distance D_c, after which the friction drops much more rapidly and the block resticks [8]. In this case, the amplitude of stick-slip decreases continuously with pulling speed, and the transition to steady sliding is continuous [16].

Much of the current theoretical understanding of the frictional properties of boundary lubrication has been the result of large scale atomistic modeling of these systems. In a series of molecular dynamics simulations, Robbins and Thompson [10] considered the case of a lubricant a few molecular layers thick consisting of spherical or chainlike molecules between two crystalline plates. The system was driven in two separate ways: first they applied a constant relative shear force, and second a spring of stiffness k was attached to one of the plates and pulled at the other end with constant velocity V. The second case mimics the experimental setup of Yoshizawa and Israelachvili illustrated in Fig. 1, and in this regime the simulations exhibit a crossover from stick-slip to steady sliding as a function of V as observed experimentally. Based on their simulations, Robbins and Thompson concluded that the stick-slip dynamics could be understood in terms of a dynamical shear melting of the lubricant layer. That is, when the surfaces were stuck to one another, the lubricant molecules were in a solid (though not necessarily crystalline) phase, while the onset of relative motion was associated with a melting transition, accompanied by an increase in the thickness of the layer and a sharp decrease in the Debye-Waller factor from a value which is characteristic of solids, to a value which is characteristic of liquids. The related case of adsorbed molecules on a surface was considered by Persson, who also concluded that shear melting played an important role in the transition [11].

The stop-start experiments of Yoshizawa and Israelachvili [5] are one of the strongest experimental indications that stick-slip behavior is associated with some sort of melting transition. The experiments consist of three stages. First, the black is pulled with velocity $V_1 > V_c$, i.e., in the steady sliding regime. Second, the pulling is abruptly discontinued for a time t_s. Third, pulling is reinitiated at the initial speed V_1. When the spring force $F(t)$ is monitored, it is observed experimentally that for stopping times $t_s < t_N$, F returns smoothly to the value it had taken prior to the stopping interval, while for $t_s \geq t_N$ the system initially remains stuck, producing a "stiction spike" ΔF in $F(t)$, before the force returns to the value it had taken prior to the stopping interval. Figure 3(a) illustrates the experimental data for ΔF as a function of stopping time t_s. The sharp onset at $t_s = t_N$ is referred to as the nucleation time of the frozen state.

Finally we note that the stop-start experiments is an additional situation in which the results of boundary lubrication and dry friction experiments differ qualitatively. In the case of dry friction, stop-start experiments such as those described above result in a stiction spike which increases logarithmically with time, with no sharp crossover analogous to t_N [17].

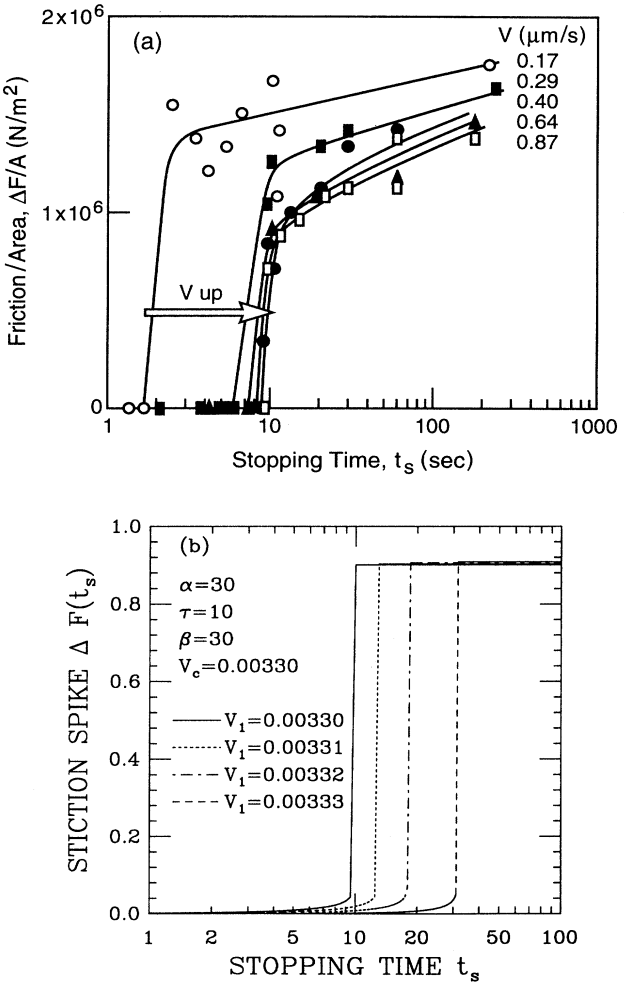

FIG. 3. The height of the stiction spike ΔF as a function of the stopping time t_s in the stop-start experiments. (a) Experimental data from Ref. [5] for hexadecane at $T = 17\,^{\circ}\mathrm{C}$. (b) Corresponding numerical results at the parameter values indicated. In both the experimental and numerical curves, there is a sharp increase in ΔF at a characteristic stopping time. At least for these parameter values, the characteristic time appears to be somewhat more sensitive to velocity in the model than is the case in the experiment.

III. RATE AND STATE LAW FOR BOUNDARY LUBRICATION

In this section we propose a constitutive relation to describe the frictional properties of boundary lubrication. The contact area is small enough and the mass is rigid enough that elastic deformation of the slider block in Fig. 1 is negligible. Thus the dynamical behavior is reasonably well represented by motion of a single degree of freedom, and the equation of motion is simply given by

$$m\ddot{U} = -k(U - Vt) - F_0 \ , \tag{1}$$

where U is the displacement of the block, dots denote time derivatives, and the parameters are defined as in the schematic experimental diagram (Fig. 1). In principle, the net friction frictional force F_0 at any given moment in time will depend on the details associated with the microscopic properties of the lubricant. However, in cases where the system is sufficiently large to be self-averaging, an effective dependence of the friction on macroscopic variables such as time, displacement, and velocity of the sliding block will emerge.

As in the solid on solid case, our relation will depend on the rate $\dot{U}$ and state θ of the system. However, our θ will be at least loosely associated with the degree to which the lubricant layer is melted [18]. We begin by writing the friction forces F_0 in its fully dimensional form as follows:

$$F_0 = \theta + \beta\dot{U} \ , \tag{2}$$

where

$$\dot{\theta} = \frac{(\theta - \theta_{\min})(\theta_{\max} - \theta)}{\tau} - \alpha(\theta - \theta_{\min})\dot{U} \ . \tag{3}$$

We constrain θ to lie between $\theta_{\min}$ and $\theta_{\max}$, corresponding to the fully melted and frozen states of the lubricant, respectively. The friction force F_0 corresponds to the maximum static friction when $\dot{U}=0$, and the dynamic friction when $\dot{U} \geq 0$. If the block were to slip backwards ($\dot{U} < 0$), then we would have to replace $\dot{U}$ in (3) with its absolute value and define

$$F_0^{\pm} = \pm\theta + \beta\dot{U} \ , \tag{4}$$

with F_0^+ as above corresponding to the dynamic friction when $\dot{U} > 0$, F_0^- corresponding to the dynamic friction when $\dot{U} < 0$, and $\pm\theta$ corresponding to upper and lower bounds on the static friction. However, as described below we will choose $\theta_{\min}$ and $\theta_{\max}$ in a manner which prevents the block from sliding backwards, which is typically the case in experiments.

Physically, the equations can be interpreted as follows. The friction F_0 depends both on the degree to which the system is melted θ, and the relative velocity $\dot{U}$ of the interface. The simplest expression we can choose corresponds to a linear dependence on θ as well as a linear dependence on $\dot{U}$, the latter of which has the familiar form associated with a simple fluid with viscosity β. When $\dot{U}=0$, $F_0=\theta$ is the maximum state friction. Here the magnitude of the static friction threshold depends on time but is bounded above by $\theta_{\max}$, while $\theta_{\min}$ corresponds to a lower bound on both the static and dynamic friction.

Equation (3) describes the evolution of the state variable. Alone, the first term on the right hand side describes the behavior when the mass is at rest ($\dot{U}=0$). Experimentally stick-slip is only observed at temperatures T at which the film at rest is frozen. Therefore, we have constructed this term so that the two $\dot{U}=0$ stationary states correspond to an unstable melted state $\theta=\theta_{\min}$, and a stable frozen state $\theta=\theta_{\max}$, such that from any initial state $\theta \neq \theta_{\min}$ the film will tend to freeze at a characteristic rate proportional to τ^{-1}. More generally, at higher temperature one expects a transition at which $\theta=\theta_{\min}$ becomes stable, and $\theta=\theta_{\max}$ is no longer a fixed point. However, because we are interested in the dynamical (as opposed to thermal) crossover from stick-slip to stable sliding we will not consider explicit temperature dependence here. The second term on the right hand side of (3) is the simplest term which can be used to describe the tendency of the film to melt as a consequence of the relative shear. As we will see shortly, $1/\alpha$ plays the role of a characteristic melting length (i.e., slip distance over which the melting transition takes place). Finally, we note that the forms of Eqs. (2) and (3) were chosen in an effort to construct a minimal model which is consistent with various qualitative aspects of the experiments. We expect that certain higher order terms may be found to be relevant upon more detailed quantitative comparison with the data.

In the next section we will focus on solutions obtained when Eqs. (2) and (3) represent the friction law in the experimental setting illustrated in Fig. 1. We assume the motion of the slider block can be represented by a single degree of freedom, with center of mass position $U(t)$ as described by Eq. (1). For convenience we set the values of the parameters $\theta_{\min}$ and $\theta_{\max}$ in a manner which rules out the possibility of backwards sliding, since backwards sliding has been observed only rarely in experiments, and only in the underdamped regime. In our case, a sufficient condition to rule out the possibility of backwards sliding is $\theta_{\max} < 3\theta_{\min}$, which is a reasonable assumption since the static and dynamic friction, roughly $\theta_{\max}$ and $\theta_{\min}$, respectively, typically differ by a factor of roughly 2 [19] (i.e., $\theta_{\max} \approx 2\theta_{\min}$). This particular criterion is obtained by considering the bounding case where the block reaches the friction threshold at $t=0$ with the maximum value $\theta(t=0)=\theta_{\max}$, and the sliding friction is simply taken to be $\theta_{\min}$, which is a lower bound on values obtained from Eq. (2). In that case, when $\theta_{\max} < 3\theta_{\min}$ in the solution of (1) with F_0 given by $F_0^{\pm}$ in Eq. (4) the block will slip and subsequently restick when $\dot{U}=0$ without sliding backwards.

Finally, before we solve for the motion we will simplify our notation by reducing the equations to dimensionless form. First, we rescale θ so that it lies in the unit interval. That is, $\theta' = (\theta - \theta_{\min})/(\theta_{\max} - \theta_{\min})$, so that $\theta'=0$ corresponds to the fully melted state, while $\theta'=1$ corresponds to the fully frozen state. Second, we rescale time so that $t' = t/\sqrt{m/k}$. As a result in the dimensionless equation the characteristic period of the mass spring sys-

tem in the absence of friction is 2π, and the characteristic slipping time of a mass subject to constant dynamic friction is π. Finally, we shift the origin and rescale the displacement according to $U'=(k/\mathcal{F}_0)[U-(\theta_{\min}/k)]$, where $\mathcal{F}_0=\theta_{\max}-\theta_{\min}$. This has the effect of (i) absorbing an overall additive constant in the friction law, and (ii) setting the characteristic slip distance in the absence of sliding friction and in the limit of infinitesimal pulling speeds equal to two.

In these units, there are four remaining variables, which are determined by materials properties of the system and external parameters such as the pulling speed. In terms of the original variables these are

$$\begin{aligned} V' &= V\sqrt{mk}\,/\mathcal{F}_0\ , \\ \beta' &= \beta/\sqrt{mk}\ , \\ \tau' &= \tau\sqrt{k/m}\,/\mathcal{F}_0\ , \\ \alpha' &= \alpha\mathcal{F}_0/k\ . \end{aligned} \tag{5}$$

Dropping the primes, the equations describing the motion of the slider mass become

$$\ddot{U}=-(U-Vt)-F_0\ , \tag{6}$$

where the friction is

$$F_0=\begin{cases}(-\infty,\theta], & \dot{U}=0\\ \theta+\beta\dot{U}, & \dot{U}>0\end{cases} \tag{7}$$

and

$$\dot{\theta}=\frac{\theta(1-\theta)}{\tau}-\alpha\theta\dot{U}\ . \tag{8}$$

With four remaining parameters it is still possible to obtain a variety of behaviors from these equations. Here we will focus on the qualitative behavior of the model in regimes which appears to best resemble the overdamped experimental data of Yoshizawa and Israelachvili. Additional experiments are necessary to quantitatively test these equations and to obtain a detailed fit of Eqs. (6)–(8) although preliminary results are quite promising [20].

IV. COMPARISON WITH EXPERIMENT

In this section we discuss solutions of Eqs. (6)–(8). We focus on specific experimentally observed phenomena discussed in Sec. II. In Sec. IV A we discuss the transition from stick-slip to steady sliding. In Sec. IV B we discuss stop-start experiments in the steady sliding regime. We will also discuss in Sec. IV C some approximate analytical solutions for the pulse shapes and transition velocity.

A. Transition from stick-slip to steady sliding

Like the experimental system, our model exhibits a transition from stick-slip to steady sliding at a critical velocity V_c. Figure 2(b) illustrates the value of the pulling spring force $F=-(U-Vt)$ in Eq. (6) which exhibits similar qualitative behavior to the experimental data of Yoshizawa and Israelachvili [5], illustrated in Fig. 2(a). For $V<V_c$ the mass alternates between sticking, where the spring force increases linearly with time, and slipping, where the spring force drops sharply, relaxing in an exponential-like decay until at some later time it resticks abruptly. For both the model and experimental parameters shown here, the duration of the slip exceeds the characteristic slip time of an underdamped spring-block system (π in our scaled units), corresponding to the "overdamped" regime. For our results this is not too surprising given the large value of β, chosen here because large values of β give the best fits to experiments. However, in the model it is also possible to obtain long slip times in regimes where $\beta<2$, which marks the crossover from overdamped to underdamped behavior in a damped harmonic oscillator with no state dependence. In both the model and experiments the transition from stick-slip to steady sliding is discontinuous. Of course, because the model corresponds to a single deterministic degree of freedom, it will not exhibit the intermittent behavior sometimes observed near the transition in the experimental system. However, like the experimental data, in the model the duration of slip becomes longer as the pulling speed increases. There are also parameters ranges, for both the model and experiment, in which the systems exhibit short, or underdamped pulses, in which the slip time is of order π. This regime will be addressed in detail in a later publication.

B. Stop-start experiments

As described in Sec. II, in the stop-start experiments the block is pulled at a velocity $V_1>V_c$, then pulling is ceased for a stopping time t_s, after which pulling at the original speed is resumed. The height of the stiction spike $\Delta F(t_s)$ refers to the difference between the maximum spring force observed after pulling is resumed and the steady state force at velocity V, and is illustrated for the experimental system in Fig. 3(a). Note that $\Delta F(t_s)$ increases sharply at a time $t_s=t_N$. This suggests that if $t_s<t_N$ the system remains melted throughout the stopping interval, and smoothly resumes sliding at velocity V when pulling begins again. In contrast, when $t_s>t_N$, the system has time to freeze during the stopping interval. In that case, when the pulling is resumed the block will stick until the force reaches the friction threshold (determined by the extent to which the system has frozen). This in turn determines the maximum value of the friction, before returning to the steady sliding state. In this sense t_N is associated with the nucleation time for the frozen state.

It is straightforward to repeat this experiment for our model. We solve Eqs. (6)–(8) with

$$V=V(t)=\begin{cases}V_1, & t<0\\ 0, & 0\le t\le t_s\\ V_1, & t>t_s\end{cases} \tag{9}$$

and constrain the pulling speed such that $V_c<V_1<(\alpha\tau)^{-1}$, so that the steady state value of θ [Eq. (10) below] is nonzero [21]. The results are shown in Fig. 3(b). While we always detect some nonzero $\Delta F(t_s)$, as in the experiment, there is a sharp onset in $\Delta F(t_s)$ at a stopping time $t_s=t^*$.

C. Analytical solutions

While the system that we study is in principle very simple—a single rigid block driven by a spring and sliding on a surface subject to the friction F_0—Eqs. (6)–(8) are sufficiently nonlinear that they defy exact solutions except in special circumstances. However, it is still possible to piece together a combination of exact and approximate solutions, each of which is valid over some limited time interval, to describe with high accuracy the stick-slip motion as well as the transition to steady sliding. Below we consider four different regimes. The first, and simplest case is the steady state behavior, which is applicable when the system slides at constant velocity. This is followed by three different cases which describe the behavior of θ during different portions of the stick-slip pulse: the growth of θ corresponding to the freezing transition when the block is at rest, the initial stages of sliding which corresponds to a rapid decrease of θ in a "slip-melting" transition, and the middle and later stages of sliding and resticking in which θ slowly increases at a rate which depends on the slip speed.

Solutions of the equation of motion (6) in the three cases describing different parts of the stick-slip pulses are straightforward to calculate and can be combined to obtain an excellent match to our numerical solutions of the full equation of motion in the overdamped regime (see Fig. 5). Perhaps the most useful aspect of the analytical solution is the insight it provides regarding the nature of the state variable in each of the four different regimes, where in each case θ may depend most directly on different macroscopic variables—time, position, and velocity. Finally, on the basis of these solutions, it is also possible to extract a criterion for the transition from stick-slip to steady sliding, that is, a critical velocity V_c.

Velocity-weakening steady sliding

First we consider the steady state value of θ, corresponding to constant relative velocity $\dot{U}=V$ at the interface. This case corresponds to the behavior of θ in the steady sliding regime, i.e., $V \geq V_c$. As $t \to \infty$ we have $\dot{\theta}=0$ and

$$\theta = \begin{cases} 1-\alpha\tau V, & V<(\alpha\tau)^{-1} \\ 0, & V \geq (\alpha\tau)^{-1} \end{cases} \tag{10}$$

so that θ depends explicitly on the velocity of the block, and is described by a piecewise linear velocity-weakening law. Of course, the form of Eq. (8) implies that evolution of θ to the exact steady state value given in (10) from some other initial value will take infinitely long. However, at sufficiently long times it is a good approximation. Assuming $(\alpha\tau)>\beta$ (which is required to obtain stick-slip at slower pulling speeds), when Eq. (10) is substituted into the friction law (7), we obtain

$$F_0^{ss} = \begin{cases} 1-(\alpha\tau-\beta)V, & V \leq (\alpha\tau)^{-1} \\ \beta V, & V>(\alpha\tau)^{-1} \end{cases} \tag{11}$$

(where ss denotes steady sliding) corresponding to linear velocity-weakening friction for $V<(\alpha\tau)^{-1}$ crossing over to linear velocity strengthening friction when $V \geq (\alpha\tau)^{-1}$.

For all of the parameters we have investigated, the transition from stick-slip to steady sliding occurs at velocities which are somewhat less than $(\alpha\tau)^{-1}$, i.e., on the velocity-weakening branch of the steady state friction. Note that in the steady sliding regime $\ddot{U}=0$ so that the steady state spring force is simply equal to the steady state friction. This implies that a measurement of the spring force as a function of pulling speed when $V>V_c$ will exhibit velocity-weakening over a range of velocities in the neighborhood of the transition (a behavior which has been observed experimentally [12]), though in some cases the range of pulling speeds over which this behavior is observed is very small.

Solidification at zero slip velocity

Second we consider the case which describes freezing of the lubricant when the system is at rest: $\dot{U}=0$ at time $t=0$, with $\theta(t=0)=\theta_0$. This analysis applies to the stuck portions of each stick-slip pulse, as well as to periods in the stop-start experiment in which the system is at rest.

Solving Eq. (8) with these initial conditions yields the exact solution for the state variable:

$$\theta(t) = \frac{\theta_0}{\theta_0+(1-\theta_0)e^{-t/\tau}} . \tag{12}$$

This functional form implies that when $\theta_0 \ll 1$, $\theta(t)$ exhibits a well-defined crossover from a value near its initial (small) value to a value near unity at a finite characteristic time. In particular, Eq. (12) increases exponentially at small times, while at large times $\theta(t)$ saturates at unity. Using (12) we can estimate the time at which $\theta(t)$ crosses over from its short time to long time behavior. In particular, the time t required for the system to achieve a value of, say, $\theta=\frac{1}{2}$ is roughly

$$t^* = \tau \ln\left[\frac{1-\theta_0}{\theta_0}\right] \approx -\tau \ln\theta_0 . \tag{13}$$

In other words, the nucleation time where the lubricant crossover from a small value of θ to a value of order unity depends linearly on the parameter τ and logarithmically on the initial value θ_0.

The well-defined crossover time separating small and large values of $\theta(t)$ is related to the abrupt increase in the stiction spike ΔF in the stop-start experiments. In particular, a crude estimate of $\Delta F(t_s)$ is obtained by relating the stiction spike to the difference between the static friction $\theta(t_s)$ obtained from Eq. (12) at the end of the stopping interval, and the steady state friction during sliding, given by $F_0^{ss}=\theta^{ss}+\beta V$, where $\theta^{ss}=\theta_0=1-\alpha\tau V$ is also taken to be the approximate initial value of $\theta(t)$ at the onset of solidification in Eq. (12). Then, the fact that $\theta(t)$ exhibits a sharp crossover at t_s of order t^* suggests that ΔF will also increase sharply at this characteristic time. However, while this form of t^* agrees qualitatively with the results of the full equations of motion illustrated in Fig. 3(b), in terms of both the existence of a sharp crossover and the specific manner in which the crossover

scales with velocity, we have found that good quantitative results for the form of $\Delta F(t_s)$ and the value of t^* require much more detailed analysis of Eqs. (6)–(8) which we have performed but which is too cumbersome to be included explicitly here. In particular, to obtain the more accurate solution we must take into account corrections associated with resticking of the block at the beginning of the stopping period (or slowing down for shorter stopping intervals), and corrections associated with the actual time the block spends at rest, which is not equal to t_s, but instead will be modified both by the time it takes to stop and the time it takes to increase the spring force to the friction threshold after pulling has begun again.

Finally, Eq. (12) can be used to determine the duration of the sticking portion of a stick-slip pulse, such as those illustrated in Figs. 2(b) and 4. In particular, if the displacement of the block at the beginning of the sticking interval is taken to be $U(t=0)=U_0$ and $\theta(t=0)=\theta_0$, then the sticking time satisfies $Vt-U_0=\theta(t)$. (Note that U_0 and θ_0 are not adjustable parameters. Instead, because the stick-slip solution is periodic, their values will be fixed for our solution by the values of θ and the spring force at the end of the slip pulse.) If $\theta(t)\approx 1$ at the end of the interval, which is strictly true in the limit of infinitesimal pulling speeds, and is a good approximation for the overdamped pulses shown in Figs. 2(b) and 4, then sliding initiates at time

$$t=t_1\approx(1+U_0)/V\ . \tag{14}$$

The time t_1 which marks the end of the stuck portion of the stick-slip pulse is marked explicitly on the solution illustrated in Fig. 5, where we compare the approximations and analytical results of this section to the numerical solution of the complete equations of motion.

Slip-weakening during the initial stages of sliding

Third we consider the case where the interface is just beginning to slip at time $t=t_1$, which we have calculated above. Again we will assume that the lubricant is initially fully frozen: $\theta(t_1)=1$, so that a system which is just beginning to slip at time t_1 will have $\dot{U}(t_1)=0$ and

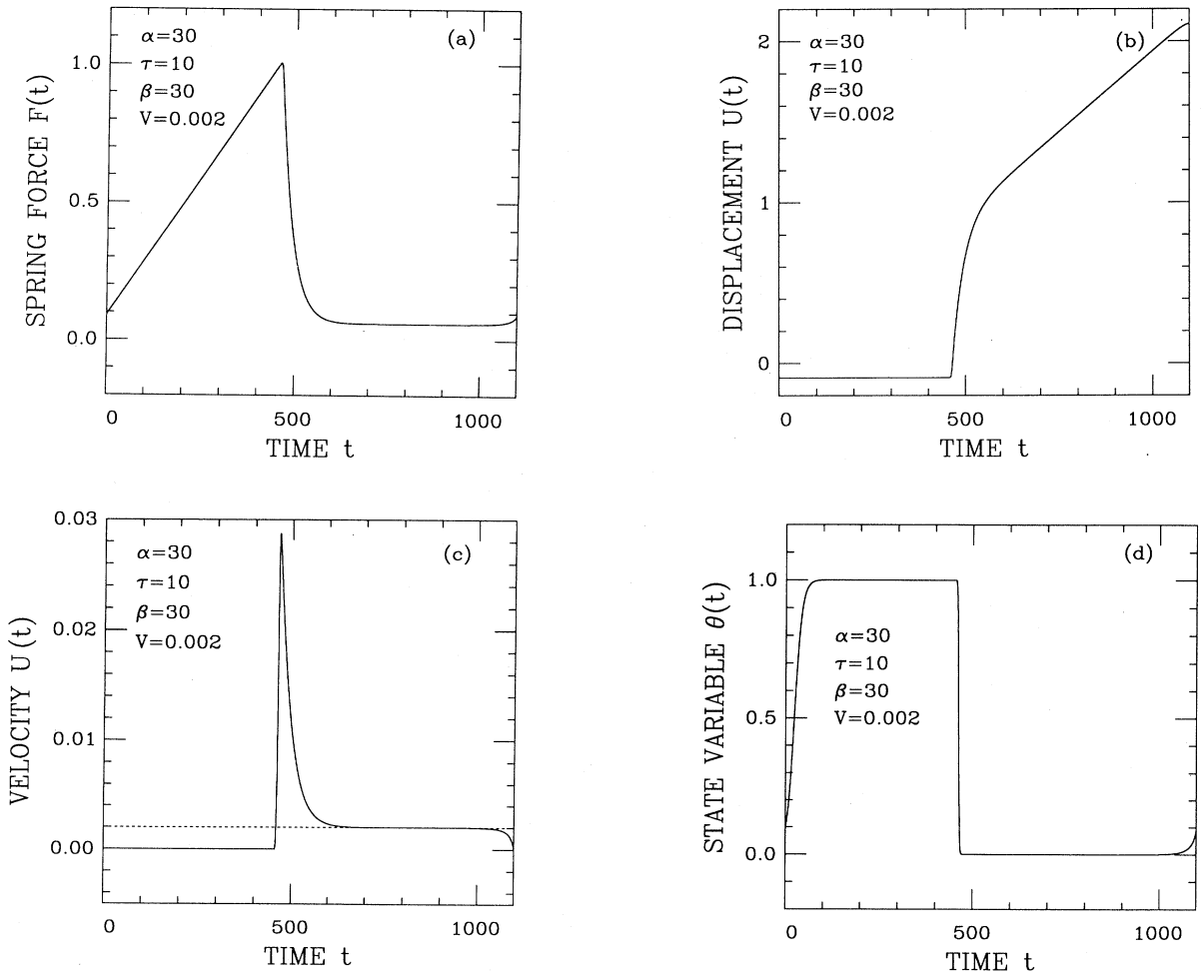

FIG. 4. (a) Spring force $F(t)=-(U-Vt)$. (b) Displacement $U(t)$. (c) Velocity $\dot{U}(t)$ (where the pulling speed V is indicated by the dotted line). (d) State variable $\theta(t)$ for a single period of the periodic stick-slip motion are illustrated. The parameter values are the same as those in Fig. 2(b).

$U(t_1) \equiv U_1$, where $U_1 = U_0$, the same as the initial value taken above, since the displacement does not change while the block is at rest.

At the initial stages of slip, when $\alpha \gg 1/\tau$ the first term on the right hand side of (8) can be ignored, so that it is a good approximation to write

$$\dot{\theta} = -\alpha\theta\dot{U} , \tag{15}$$

from which we obtain

$$\theta = e^{-\alpha(U-U_1)} . \tag{16}$$

Here the state variable θ depends explicitly on slip

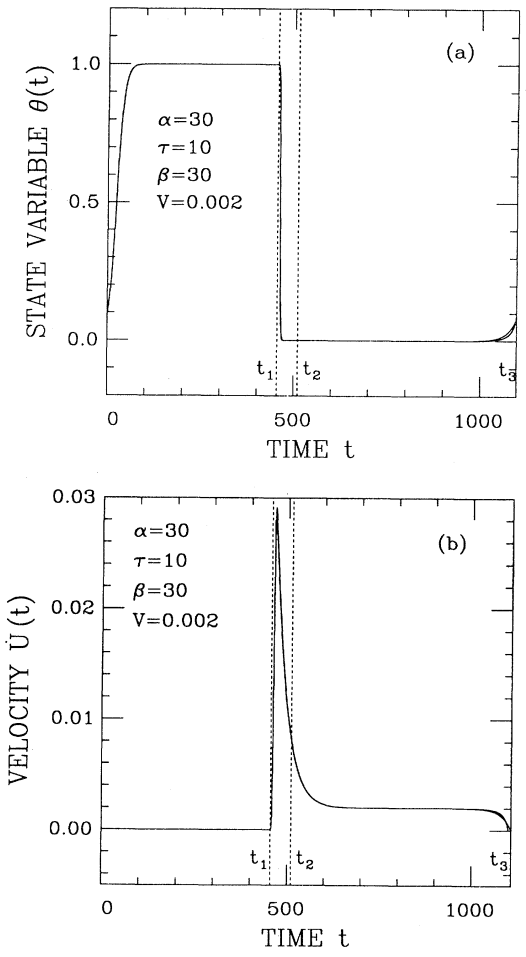

FIG. 5. A comparison between the full solution of the equations of motion (as in Fig. 4), and the analysis presented in Sec. IV C (both shown here) reveals that the two solutions are almost indistinguishable. (a) State variable θ and (b) illustrates the velocity for a single period of the motion. Over the time interval $[0,t_1]$ the state variable θ undergoes a freezing transition, which takes place over a characteristic time interval, over the interval $[t_1,t_2]\theta$ decreases rapidly, but continuously, over a characteristic slip distance (i.e., exhibits slip-weakening), over the interval $[t_2,t_3]\theta$ begins to freeze at a rate which depends both on time and slip velocity. The intermediate times t_1 and t_2 are marked with dotted lines, and the initial and final times correspond to the limits of the x axis shown.

$\Delta U = U - U_1$, and "melts" over a characteristic distance $1/\alpha$.

Using an additional approximation it is possible to obtain a closed form analytical solution for $U(t)$ which agrees with the numerical results at the very beginning of this branch of the solution. For a piecewise linear approximation to Eq. (16)

$$\theta = \begin{cases} 1-\alpha(U-U_1), & U-U_1 < \alpha^{-1} \\ 0, & U-U_1 \geq \alpha^{-1} \end{cases} \tag{17}$$

during the initial stages of slip we solve

$$\ddot{U} = (\alpha-1)U + Vt - \beta\dot{U} - (1+\alpha U_1) \tag{18}$$

to obtain

$$U(t) - U_1 = A(t-t_1) + B + Ce^{\Gamma_+(t-t_1)} + De^{\Gamma_-(t-t_1)} \tag{19}$$

where $\Gamma_\pm = -\beta/2 \pm [\alpha - 1 + (\beta/2)^2]^{1/2}$ and the constants are straightforward to obtain: $A = -V/(\alpha-1)$, $B = -\beta V/(\alpha-1)^2$, $C = (-A + B\Gamma_-)/(\Gamma_+ - \Gamma_-)$, and $D = -(B+C)$. Note that stick-slip behavior requires $(\alpha-1) > 0$, which is necessary to obtain the initial slip-weakening instability in (18) that leads to exponential growth of the Γ_+ mode in the solution (19). In particular, this mode soon dominates the behavior, and the solution grows exponentially at a rate given by $\Gamma_+ \approx \alpha/\beta$ when $\alpha \gg 1$ and $(\beta/2)^2 \gg \alpha$.

While the solution (19) provides a good approximation to the full equation of motion as the block just begins to become unstuck, the linear approximation (17) to the exponential slip-weakening law (16) breaks down before we move to the next branch of the solution. In contrast, a numerical solution using the exponential slip-weakening law in (16) to approximate the behavior of the state variable θ yields a solution which is essentially indistinguishable from the full numerical solutions of Eqs. (6)–(8) in the time interval from t_1 to t_2 in Fig. 5. The solutions agree well up to the point where θ assumes some minimum value, which is the only adjustable parameter we allow in fitting our approximations to the full solution. Here the minimum corresponds to $\theta = 5 \times 10^{-12}$, so that the lubricant is essentially fully melted. Given this minimum value of θ for the fit, it is clear that the solution to the linearized equation (18) must break down, since when θ is that small the exponential in (16) is well beyond the linear regime. However, the agreement between the full solution and the solution based on the exponential slip-weakening law in the time interval $[t_1,t_2]$ illustrated in Fig. 5 is excellent and thus verifies that slip-weakening is the mechanism best describing the state variable during this stage of the slip.

The origin of the characteristic distance for melting comes from the fact that $\dot{\theta}$ is linearly coupled to the relative velocity in Eq. (15) so that $d\theta/\theta \propto dU$. Additional temporal dependence of the melting transition may become relevant in regimes where the first term on the right hand side in Eq. (8) is non-negligible or when Eqs. (7) and (8) are modified to include higher order terms.

However, it is noteworthy that the existence of a characteristic distance over which the friction decreases in boundary lubrication is indirectly supported by the experiments of Reiter *et al.* [22] which explore the crossover from elastic to dissipative response in similar systems. They find that there is a transition from a fully elastic response to a partially dissipative response (associated with stick-slip), which depends on the displacement amplitude for very small displacements, and is independent of frequency. While the typical displacements in these experiments are orders of magnitude less than those in Ref. [5], in the case of Reiter *et al.* the distance $1/\alpha$ over which a slip-weakening transition (which may or may not correspond to a melting transition in their case) takes place in the film corresponds to a microscopic length, of order a few nm.

Partial refreezing at slow speeds

When the damping β is sufficiently large the peak velocity is reached at some point during the melting transition, at which point $\dot{U}$ begins to decay at a rate governed by the parameter β. In the next branch of the solution (times between t_2 and t_3 in Fig. 5) the decay continues until the velocity of the block approaches the pulling speed V. Simultaneously, during this interval θ begins to increase. It requires a characteristic time interval (which depends on the pulling speed) for θ to begin to make a significant contribution to the friction, which ultimately causes the block to restick.

In the interval $[t_2,t_3]$, which begins the moment the lubricant has reached the maximally melted state and extends through the moment the block resticks, it is a good approximation (second line) to the full equation (first line) to write

$$\dot{\theta}=\frac{\theta(1-\theta)}{\tau}-\alpha\theta\dot{U}$$
$$\approx\theta(\tau^{-1}-\alpha V)\ , \tag{20}$$

so that for $\theta=\theta_2$ at $t=t_2$ we have

$$\theta=\theta_2\exp[(1-\alpha\tau V)(t-t_2)/\tau]$$
$$\equiv\theta_2\exp[(t-t_2)/\tau']\ . \tag{21}$$

The exponential growth of θ with time corresponds to the onset of solidification from the melted state, at a rate $1/\tau'\equiv(1-\alpha\tau V)/\tau$ which is decreased by a factor of $(1-\alpha\tau V)$, compared to the corresponding rate $1/\tau$ associated with the initial stages of solidification in (12) when the system is stationary.

In Eq. (20) we have made two simplifying approximations. First, we have dropped a factor of $(1-\theta)$ in the first term of the right hand side, which is a good approximation when θ is small (as will typically be the case after the slip-melting transition). In addition, we have replaced $\dot{U}$ in the second term with V. Even though $\dot{U}$ is somewhat larger than V at the earliest stages of this branch of the solution (time t_2 in Fig. 5), the approximation gives an excellent fit to the full numerical solution. This will be true as long as β is not too large, so that the velocity decays to $\dot{U}\approx V$ by the time (roughly τ') that the exponential growth of θ begins to play a significant role.

If $U(t_2)=U_2$ and $\dot{U}(t_2)=\dot{U}_2$ (where we take these initial conditions from the numerical solution to the exponential slip-melting transition discussed above), using this approximation we obtain a solution of (6) of the form

$$U(t)=Vt-\beta V+Pe^{(t-t_2)/\tau'}+Qe^{\lambda_+(t-t_2)}+Re^{\lambda_-(t-t_2)}\ , \tag{22}$$

where $\lambda_\pm=-\beta/2\pm[(\beta/2)^2-1]^{1/2}$, $P=-\theta_2/(1+\beta/\tau'+1/\tau'^2)$, $Q=[\dot{U}_2-V-P/\tau'-\lambda_-(U_2+\beta V-Vt_2-P)]/(\lambda_+-\lambda_-)$, and $R=U_2+\beta V-Vt_2-P-Q$. We obtain the velocity simply by differentiating Eq. (22)

$$\dot{U}(t)=V+\frac{P}{\tau'}e^{(t-t_2)/\tau'}+Q\lambda_+e^{\lambda_+(t-t_2)}$$
$$+R\lambda_-e^{\lambda_-(t-t_2)}\ . \tag{23}$$

This branch of the solution agrees well with the results shown in Fig. 5 in the time interval $[t_2,t_3]$. While the last term in (23) does not play an important role in this branch of the solution, as V approaches V_c each of the other three terms dominates the behavior in a particular subinterval.

The initial decay from the velocity $\dot{U}_2$ to a speed $\dot{U}\approx V$ occurs at a rate which is determined primarily by the viscosity β. Because θ is initially very small, the system is simply behaving like an overdamped harmonic oscillator, which naturally relaxes to the pulling speed. Of the two exponentially relaxing modes $\lambda_\pm$, λ_+ is the slow mode, and thus sets the time scale for this initial relaxation, given roughly by $\Delta t_{\rm relax}=-1/\lambda_+\approx\beta$ when $\beta\gg1$. Note that relaxation from above, i.e., $\dot{U}\to V^+$, occurs when the coefficient $Q>0$, and corresponds to a continuing decrease in the spring force F throughout the slip, as seen experimentally [23].

If the time associated with the initial decay of the velocity is much less than the time associated with the growth of θ (i.e., when $\beta<\tau'$), there will be an intermediate interval during which the two decaying modes $\lambda_\pm$ have become negligibly small, while the exponentially growing term (which is proportional to θ) does not yet play a significant role. During this period $\dot{U}\approx V$. Furthermore, because τ' increases as $V\to V_c$ the duration of this intermediate interval will increase with increasing pulling speed.

Finally, while the initial exponential relaxation is controlled by the parameter β, the exponential increase of θ, which contributes to $\dot{U}(t)$ through the second term on the right hand side of (23), dominates the behavior at the end of the slip pulse. It is in fact the sharp increase in θ at a time of order τ' after this branch of the solution begins, that gives rise to the relatively abrupt return to the stuck state. The time to stop is given more precisely by estimating the time t_3 at which $\dot{U}=0$, which is obtained from (23). When $\beta<\tau'$ to a good approximation this is obtained using only the first two terms on the right hand side of (23), so that

$$t_3 - t_2 \equiv t_{\text{stop}} \approx \tau' \ln\left[-\frac{V\tau'}{P}\right] . \tag{24}$$

At slower pulling speeds, or higher values of β, the approximation $\beta < \tau'$ may not be valid, and the exponential decay to the pulling speed may not be complete by the time the block resticks. Under such circumstances, an alternate formula for t_{stop} may be obtained by setting the sum of the slow mode λ_+ and the exponentially growing term to zero. In either case because the solidification rate depends on the approximate slip speed V, the length of the pulse will increase with increasing pulling speed.

To obtain the full periodic stick-slip solution, we can now return to the initial stage describing the more rapid solidification at zero slip velocity, where $\theta(t)$ increases according to (12) from the initial value θ_0, which is now fixed by $\theta_0 = \theta(t = t_3)$. Similarly the value of U_0 in Eq. (14), which determines the length of the sticking interval for the periodic solution, is simply $U_0 = U(t_3) - Vt_3$. In the overdamped regime, because θ returns to a value near unity before the block slips again, arbitrary initial conditions (with the exception of an initial condition which exactly corresponds to the unstable steady sliding state) converge very rapidly to the periodic solution, essentially by the end of the first pulse.

Transition from stick-slip to steady sliding

Finally, we examine the transition from stick-slip to steady sliding. Figure 6 illustrates the numerical solutions $\theta(t)$ and $\dot{U}(t)$ obtained from the full equations of motion, Eqs. (6)–(8), as the velocity is increased from a value just below V_c for $t < 0$ to a value just above V_c for $t > 0$. The time interval shown begins with the last complete slip pulse for $V < V_c$, which agrees well with the analytical results in this section, and extends through the crossover to steady sliding where $\theta(t)$ approaches the steady state value described by (10). Here the transition is clearly associated with a failure of the block to come to rest in the last part of the slip pulse described by the partial refreezing at slow speeds, as opposed to some other scenario such as a failure of the system to refreeze once it has stuck (which might then be associated with a failure of our solution during the time interval associated with slip weakening). In particular, when $V > V_c$ we find that $\theta(t)$ first departs from our analytical results in the branch described by (21). Rather than the slow but steady exponential increase in θ which is predicted by (21), at some point θ turns around and begins to decrease, ultimately approaching the steady state value. From (8) it is clear that θ will decrease rather than increase when

$$\frac{(1-\theta)}{\tau} < \alpha \dot{U} . \tag{25}$$

This provides one check of the self-consistency of our stick-slip solution.

With $\theta(t)$ given by Eq. (21), and $\dot{U}(t)$ given by (23), we estimate the time t_3' at which our solution will fail in terms of the breakdown time t_B. In particular, if $t_B < t_{\text{stop}}$ (i.e., if self-consistency of the solution fails before this branch of the solution is complete and the block has come to rest) the stick-slip solution given here is no longer valid, and instead the system crosses over to a steady sliding state [24]. Using the same approximations that led to t_{stop} (i.e., assuming $\beta \ll \tau'$), the time t_B that this occurs is given by

$$t_3' - t_2 \equiv t_B = \tau' \ln\left[-\frac{\tau}{P(\tau' + \beta + 1/\tau' - \alpha\tau)}\right]$$

$$\approx \tau' \ln\left[-\frac{\tau}{P(\tau' + \beta - \alpha\tau)}\right] , \tag{26}$$

where P is the same constant that appears in Eq. (22). The stick-slip solution is no longer self-consistent if $t_B < t_{\text{stop}}$, and there will be a transition to stable sliding. Thus we obtain a formula for the critical velocity:

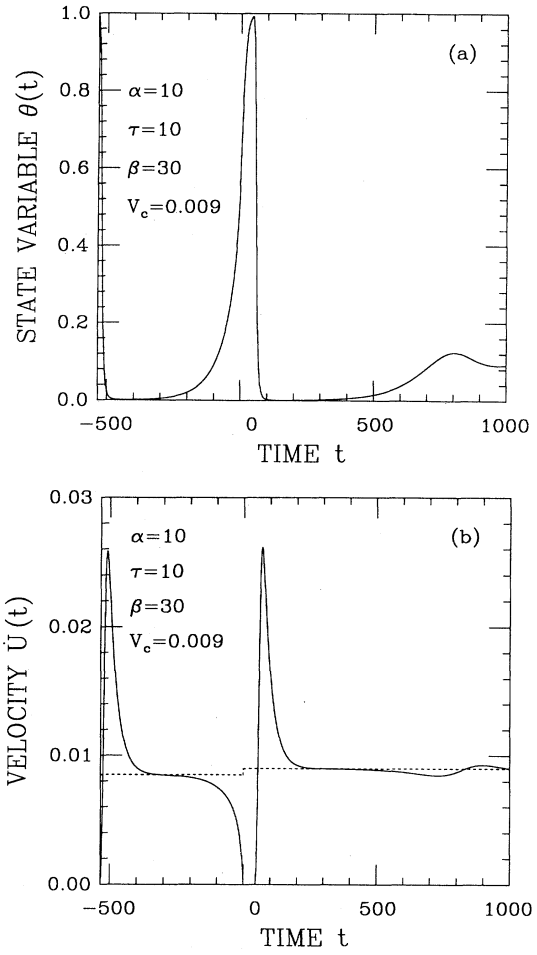

FIG. 6. The transition from stick-slip to steady sliding is associated with a breakdown in the self-consistency of the analytical solution over the time interval $[t_2, t_3]$ in Fig. 5 which is associated onset of freezing at slow speeds in the stick-slip solution. Here the pulling speed changes from a value just below V_c to a value slightly greater than V_c at time $t = 0$. When $V > V_c$, rather than a steady increase in θ (a) as described by (21), the solution instead approaches the steady state value given in (10). The velocity is shown in (b), where the dotted line represents the pulling speed V.

$$(\beta\alpha\tau)V_c^2-(\alpha\tau+\beta+\tau)V_c+1=0\ . \tag{27}$$

For larger values of α, where we expect our solution to be valid, this agrees well with the full equations of motion, Eqs. (6)–(8), as illustrated in Fig. 7. Since V_c is close to $(\alpha\tau)^{-1}$ in the regime where our solution is valid, we can write $V_c=(\alpha\tau)^{-1}-\epsilon$ so that to leading order in ϵ we obtain

$$V_c\approx(\alpha\tau)^{-1}-\frac{1}{\alpha^2\tau^+\alpha\tau-\alpha\beta}$$
$$\approx(\alpha\tau)^{-1}-(\alpha^2\tau)^{-1} \tag{28}$$

where the second approximation is valid when $\alpha\gg1$, and $\alpha\tau\gg\beta$.

Note that the numerical results for α vs. V_c in Fig. 7 are obtained by fixing the parameters α, β, and τ. We then set an initial pulling speed V within the stick-slip phase, and after observing many stick-slip pulses at a given V we increment the pulling speed in small steps $\Delta V=10^{-4}$ until $V\approx V_c$ defined to be the first velocity at which stick-slip is no longer observed. As a result, most of the phase boundary is accurate to within 2% of the measured V_c. For the smallest measured value of V_c (corresponding to $\alpha=4$) the step size is reduced to $\Delta V=5\times10^{-6}$ and V_c is obtained to within 6% accuracy.

Finally, while for larger values of α, V_c decreases with increasing α as predicted by (28), numerically we observe that the converse is true for the smallest values of α as illustrated in Fig. 7. In this regime the stick-slip pulses are not well described by the approximations discussed in this section. Instead the melting (i.e., reduction of θ in an individual slip-pulse) which takes place is significantly reduced, requiring different approximations of Eqs. (6)–(8) than those which have been considered here. In this case the pulses have a velocity-dependent amplitude, and a nearly velocity-independent slip-time. However, even in the absence of detailed analysis it is worth noting that some sort of a crossover at smaller values of α is expected. In particular, our observation that stick-slip requires $\alpha\tau>\beta$, that is, the existence of a velocity-weakening branch in the steady state friction in Eq. (11), implies that stick-slip should not be observed for the parameters in Fig. 7 when $\alpha\leq3$.

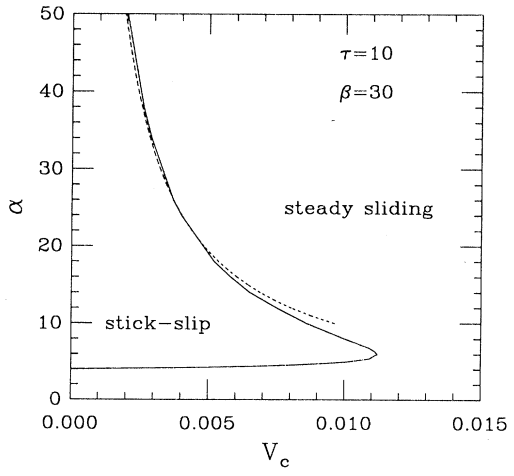

FIG. 7. Dynamical phase diagram: α vs. V_c, separating stick-slip from steady-sliding solutions. The solid line illustrates our numerical results based on the full equation of motion, and the dotted line illustrates our analytical estimate, obtained in terms of the breakdown of the self-consistent solution (as in Fig. 6). The analytical results are expected to apply when α is large.

V. CONCLUSIONS

Rate and state constitutive relations, while purely phenomenological, can provide some important guidelines for the design of mechanical systems, in terms of both materials choices and operating conditions. The work presented here represents the first step towards development of such a description for the frictional properties of boundary lubrication. In particular, we have shown that the proposed rate and state law compares well to qualitative aspects of the experiments in Ref. [5]. For both the model and experiment there is a discontinuous transition between stick-slip and steady sliding at a critical velocity V_c, the pulse shapes in the stick-slip regime are qualitatively similar, and in stop-start experiments there is a sharp crossover in the height of the stiction spike at a finite characteristic time.

Much work remains to be done in order to evaluate the particular constitutive relation we have proposed. Equations (6)–(8) were constructed to form a minimal model that captures certain key differences between the frictional properties of dry and lubricated interfaces. As a result, there is no special reason to expect that this model will adequately capture all of the subtleties associated with the detailed quantitative behavior in the lubricated case. In order to test the model quantitatively, more detailed fits to experimental data must be performed. Indeed, we have done some preliminary fits to experimental traces of individual slip pulses, and these early results show some surprisingly good quantitative agreements as the pulling speed is varied [20]. A more comprehensive effort along these lines, coupled with additional experiments, measuring both the stick-slip and steady sliding frictional properties are currently in progress and should provide much better constraints on the form of the constitutive relations than the qualitative features we have considered thus far. Measurements of the slip-pulse duration as a function of pulling speed, and the dynamical phase diagram will be especially helpful.

Our analytical studies of the equations of motion (6)–(8) provide some insights into the possible dynamical processes which may play an important role during various different stages of stick and slip. Associating the value of the state variable θ with the degree of melting of the lubricant layer, our solutions suggest that these include time-dependent freezing when the block is at rest, melting which takes place over a characteristic slip-distance during the initial stages of slip, and a time- and velocity-dependent initiation of freezing which follows the melting process, and ultimately causes the block to restick. This final process takes place at a rate which is

reduced relative to the freezing rate when the block is at rest, and ultimately it is the inability of the lubricant to refreeze during this final stage of slip which results in the transition to steady sliding at a critical pulling speed V_c.

The justification of these physical interpretations ultimately must come from microscopic models. As a first step, it will be useful to compare our results more quantitatively with results obtained from molecular dynamics simulations. In fact, in his simulations of the frictional properties of adsorbed molecules at an interface, Persson discusses the refreezing of the lubricant at slow slip speeds in terms of a velocity dependent nucleation of frozen domains [11], somewhat analogous to our interpretation of the resticking process. In the same manner used to fit our model to experimental data, it should be possible to obtain fits to simulations. Thus the constitutive relation has the potential to provide a useful link between atomistic numerical studies and experiments.

Finally, we emphasize that we have focused on a particular parameter regime of this model, which we believe most closely resembles the experiments in the overdamped regime. While the existence of stick-slip for any pulling speed required $\alpha > 1$, and $\alpha\tau > \beta$, we have made several additional choices. We have taken α to be large compared to unity, the characteristic slip distance for the undamped mass-spring system in our scaled units. This choice corresponds to selecting a small characteristic distance $\Delta U \approx 1/\alpha$ over which the slip-melting transition takes place. We have taken the viscosity β to be large, so that after the system attains its maximum speed at some point during the melting process, the velocity relaxes to the pulling speed slowly (the characteristic time in our solution is β) compared to time scales associated with the undamped mass-spring system (π in our rescaled units). Finally, we have taken τ large compared to unity as well, so that all freezing processes are slow compared to the inertial time.

When the relative sizes of these different time and length scales are altered, the behavior of the model can be quite different. While behavior which is qualitatively different from the overdamped pulses has been observed experimentally (e.g., underdamped pulses), it remains an open question to determine the extent to which these different regimes are also captured by Eqs. (6)–(8), and to determine the full range of behaviors a single lubricant system under different mechanical and environmental constraints might explore.

ACKNOWLEDGMENTS

We have profited from numerous useful discussions with James Langer, James Rice, Jacob Israelachvili, and Alan Berman. This work was supported by a grant from the David and Lucile Packard Foundation and NSF Grant Nos. DMR-9212396 and DMR-9510394.

[1] See, e.g., *Handbook of Micro/Nano Tribology*, edited by B. Bhushan (Chemical Rubber, New York, 1995).

[2] E. Rabinowicz, in *Friction and Wear of Materials* (Wiley, New York, 1965), Chap. 4.

[3] S. Granick, Science **253**, 1374 (1991).

[4] J. N. Israelachvili, P. M. McGuiggan, and A. M. Homola, Science **240**, 189 (1988); M. L. Gee, P. M. McGuiggan, J. N. Israelachvili, and A. M. Homola, J. Chem. Phys. **93**, 1895 (1990); H. Yoshizawa, P. McGuiggan, and J. N. Israelachvili, Science **259**, 1305 (1993).

[5] H. Yoshizawa and J. N. Israelachvili, J. Phys. Chem. **97**, 11 300 (1993).

[6] In A. L. Ruina, J. Geophys. Res. **88**, 10359 (1983). A rate and state law for the solid on solid case is introduced, in which the friction is $F_0 = \mu + A \ln(\dot{U}/V^*) + B \ln(\theta/\theta^*)$, with the evolution of the state variable given by $\dot{\theta} = 1 - (\theta \dot{U}/D_c)$.

[7] J. H. Dieterich, Pure Appl. Geophys. **116**, 790 (1978); J. Geophys. Res. **84**, 2161 (1979).

[8] J. R. Rice and A. L. Ruina, J. Applied Mech. **105**, 343 (1983).

[9] J. Caroli and P. Nozieres (unpublished).

[10] P. A. Thompson and M. O. Robbins, Phys. Rev. A **41**, 6830 (1990); Science **250**, 792 (1990); P. A. Thompson, G. Grest, and M. O. Robbins, Phys. Rev. Lett. **68**, 3448 (1992).

[11] B. N. J. Persson, Phys. Rev. B **48**, 18 140 (1993); **50**, 4771 (1994).

[12] A. Berman and J. N. Israelachvili, private communication.

[13] T. E. Tullis and J. D. Weeks, Pageoph. **124**, 383 (1986); L. A. Reinen, T. E. Tullis, and J. D. Weeks, Geophys. Res. Lett. **19**, 1535 (1992).

[14] T. Baumberger, F. Heslot, and B. Perrin, Nature **367**, 544 (1994).

[15] J. R. Rice and S. T. Tse, J. Geophys. Res. **91**, 521 (1986).

[16] T. Baumberger, C. Caroli, B. Perrin, and O. Rosnin, Phys. Rev. E **51**, 4005 (1995).

[17] N. M. Beeler, T. E. Tullis, and J. D. Weeks, Geophys. Res. Lett. **21**, 1987 (1994).

[18] In the case of dry friction the state variable is associated with the characteristic time required to establish a new set of microscopic constants.

[19] See, e.g., W. E. Campbell, Trans. ASME **61**, 633 (1939).

[20] These fits are based on unpublished data of A. Berman and J. N. Israelachvili.

[21] This is done to avoid the somewhat pathological behavior of the steady state value of θ at higher V, which approaches zero asymptotically with time and ultimately leads to a dependence of ΔF on the time spent in the steady sliding state before the stopping interval begins. Higher order corrections to Eq. (8) will modify the piecewise linear form of (10) and remove this problem.

[22] G. Reiter, A. L. Demirel, and S. Granick, Science **263**, 1741 (1994); G. Reiter, A. L. Demirel, J. Peansky, L. L. Cai, and S. Granick, J. Chem. Phys. **101**, 2606 (1994).

[23] If $Q < 0$ the velocity relaxes up to V from below before ultimately resticking. Such behavior would correspond to an increase in the spring force during slip, which is not seen experimentally. Such observations can be used to rule out a fraction of the possible parameter space for our model.

[24] We have not proven that there are no other solutions, but based on numerical evidence we believe it to be true.